

Title (English)	Estimating vegetation index for outdoor free-range pig production using YOLO
Running Title (English)	Estimating vegetation index for outdoor free-range pig production using YOLO
Author	Sang-Hyon OH [first_author] ¹ , Hee-Mun Park ² , Jin-Hyun Park ²
Affiliation	¹ Division of Animal Science, College of Agriculture and Life Science, Gyeongsang National University, Jinju 52725, Korea, Republic of ² School of Mechatronics Engineering, Engineering College of Convergence Technology, Gyeongsang National University, Jinju 52725, Korea, Republic of
Corresponding Author	Jin-Hyun Park (uabut@gnu.ac.kr, office: , mobile:)
ORCID	Sang-Hyon OH (https://orcid.org/0000-0002-9696-9638) Hee-Mun Park (https://orcid.org/0000-0001-5182-1739) Jin-Hyun Park (https://orcid.org/0000-0002-7966-0014)
Conflict of interest	No potential conflict of interest relevant to this article was reported.
Funding information	-
Acknowledgements	
Availability of data and material	
Author Contribution	Conceptualization: OH SH, Park JH Data curation: OH SH, Park JH Formal analysis: Park HM, Park JH Methodology: Park HM, Park JH Software: Park HM, Park JH Validation: OH SH, Park JH Investigation: OH SH, Park JH Writing - original draft: OH SH Writing - review & editing: OH SH, Park HM, Park JH
IRB/IACUC approval	The present experiment was reviewed and approved by the Institutional Animal Care and Use Committee of North Carolina A&T University (IACUC: 12-003.0).

2 **Estimating vegetation index for outdoor free-range pig production using YOLO**

3

4 Sang-Hyon OH^{1†}, Hee-Mun Park^{2†} and Jin-Hyun Park^{2*}

5

6 ¹Division of Animal Science, College of Agriculture and Life Science, Gyeongsang National
7 University, Jinju 52725, South Korea

8

9 ²School of Mechatronics Engineering, Engineering College of Convergence Technology,
10 Gyeongsang National University, Jinju 52725, South Korea

11

12 [†] Both authors contributed equally to this manuscript.

13 *Corresponding author: uabut@gnu.ac.kr

14

15 **ORCID**

16 **Sang-Hyon Oh** <https://orcid.org/0000-0002-9696-9638>

17 **Hee-Mun Park** <https://orcid.org/0000-0001-5182-1739>

18 **Jin-Hyun Park** <https://orcid.org/0000-0002-7966-0014>

19

20 **Title of the manuscript:** Estimating vegetation index for outdoor free-range pig production
21 using YOLO

22

23 **ABSTRACT**

24 The objective of this study was to quantitatively estimate the level of grazing area damage in
25 outdoor free-range pig production using a UAV with an RGB image sensor. Ten corn field
26 images were captured by a UAV over approximately two weeks, during which gestating sows
27 were allowed to graze freely on the corn field measuring $100 \times 50 \text{ m}^2$. The images were
28 corrected to a bird's-eye view, and then divided into 32 segments and sequentially inputted into
29 the YOLOv4 detector to detect the corn images according to their condition. The 43 raw
30 training images selected randomly out of 320 segmented images were flipped to create 86
31 images, and then these images were further augmented by rotating them in 5-degree increments
32 to create a total of 6,192 images. The increased 6192 images are further augmented by applying
33 three random color transformations to each image, resulting in 24,768 datasets. The occupancy
34 rate of corn in the field was estimated efficiently using YOLO. As of the first day of observation
35 (day 2), it was evident that almost all the corn had disappeared by the ninth day. When grazing
36 20 sows in a $50 \times 100 \text{ m}^2$ cornfield ($250 \text{ m}^2/\text{sow}$), it appears that the animals should be rotated
37 to other grazing areas to protect the cover crop after at least five days. In agricultural technology,
38 most of the research using machine and deep learning is related to the detection of fruits and
39 pests, and research on other application fields is needed. In addition, large-scale image data
40 collected by experts in the field are required as training data to apply deep learning. If the data
41 required for deep learning is insufficient, a large number of data augmentation is required.

42

43 **Keywords:** outdoor, pig, production, vegetation index, image analysis

44 INTRODUCTION

45 Free-range outdoor pig production is steadily increasing in the United States and Europe due
46 to the niche market strategy for small farmers, consumer antipathy to factory farm products,
47 and the trends towards environmentally friendly and animal welfare practices. Ongoing
48 research is also being conducted to support this trend [1-4].

49 One advantage of free-range outdoor pig production is that it can be operated with a small
50 capital investment. However, one of the disadvantages is that the soil can become depleted due
51 to the natural rooting behavior of pigs. If not appropriately managed, it can lead to groundwater
52 eutrophication. Accordingly, the USDA (United States Department of Agriculture) requires that
53 outdoor free-range pig production systems have at least 75% of the outdoor area covered in
54 vegetative cover, such as crops or grass [5], which is to help prevent soil erosion, improve soil
55 quality, and reduce the risk of nutrient runoff into nearby water sources.

56 As farmers who cannot accurately calculate the area covered by crops or vegetation may
57 resort to using a sacrifice area to maintain the required 75% vegetative cover, it is not
58 uncommon for pigs to be concentrated in a small area of the outdoor space while the rest is left
59 unused. However, this can lead to overgrazing and soil damage in that area, increasing the risk
60 of groundwater contamination from waste products. Therefore, it is important for farmers to
61 implement good management practices, such as rotational grazing to minimize the
62 environmental impact of outdoor pig production [6-8].

63 With the advancement of technology and science in recent years, photographing on
64 Unmanned Aerial Vehicles (UAV) is no longer a difficult and expensive task [9]. If this
65 technology were applied to outdoor free-range pig production to monitor the condition of
66 grazing areas, it would greatly help producers maintain grazing areas at recommended levels
67 without leaving them to degrade beyond repair. It may also be possible to estimate how much
68 grass a pig has consumed in a particular grazing area by comparing the color changes in the

69 captured images and the amount of pre- collected dry matter. This is particularly useful as it
70 can be challenging to gauge the amount of grass consumed by pigs as they may cause damage
71 to the grazing area.

72 YOLO (You Only Look Once) is an object detection technique utilizing deep learning in
73 images and was proposed by Redmon et al. [10], which is a system that can recognizes the
74 objects in an image and their locations at once, meaning it only needs to look at the image once.
75 Compared to the classifier-based approach of CNN (Convolutional Neural Network), YOLO's
76 network architecture is relatively simple as it directly learns the loss function that has a
77 significant impact on detection performance. YOLO also has the ability to perform real-time
78 object detection, which has been widely used in many research areas [11-14]. Figure 1 shows
79 the schematic structure of the YOLOv4 object detection system.

80 The objective of this study was to develop an algorithm to quantitatively predict the extent
81 of damaged grazing area in outdoor free-range pig production using a UAV with an RGB image
82 sensor.

83

84 **MATERIALS AND METHODS**

85

86 **Animal care**

87 The present experiment was reviewed and approved by the Institutional Animal Care and Use
88 Committee of North Carolina A&T University (IACUC: 12-003.0).

89

90 **Animals, diets, and experimental design**

91 The images used for the analysis were taken at a swine unit located within the University Farm
92 of North Carolina A&T State University (Greensboro, NC, USA; 36°4'16.63"N,

93 79°43'33.02"E). A 50×100 m² grazing area was established for twenty pregnant sows that were
94 allowed to graze pasture two weeks prior to their expected delivery date. The grazing area was
95 planted with corn crops. The climate in this location is classified as humid subtropical climate
96 (Köppen climate classification), with hot and humid summers and mild winters. The average
97 annual precipitation is around 107 cm. The sows were given access to slightly less than
98 standard National Research Council balanced rations (2-3kg/day) considering the consumption
99 of corn in the pasture, but water *ad libitum*.

100

101 **Data collection**

102 The UAV used in this study is the Phantom 2 Vision model manufactured by DJI[®] with a quad-
103 rotor system consisting of four propellers. Including a camera, the maximum takeoff weight is
104 1.3 kg, and it can fly for about 25 minutes using a 5,200 mAh lithium polymer battery (Table
105 1). It has a remote-control range of up to 300 m and is equipped with a high-resolution camera
106 sensor of 14 Megapixels and 1/2.3" size, with a fixed-focus wide-angle lens of 120° FOV and
107 a focal length of 28 mm. It is equipped with an automatic flight control device, and a 2.4 GHz
108 wireless remote controller was used for takeoff and landing as well as manual control of the
109 aircraft.

110 Ten aerial images were taken using the UAV from a height that allowed the entire grazing
111 area to be captured in a single image, from September 1st to September 13th, 2015, excluding
112 days with rain. Also, the images were captured around 10:00 AM without additional lighting,
113 with an effort made to minimize the effect of shadows caused by the sun. We tried to maintain
114 the same altitude and position using the GPS attached to the UAV. Figure 2 shows the images
115 captured by the UAV over two weeks after releasing the pigs. Each image has a size of 4,384
116 × 3,288 pixels.

117

118 **Image analysis**

119 This study aims to use only ten images captured by the UAV over a two-week period to
120 numerically represent the process of cornfield degradation caused by gestation sows, using the
121 degree of corn occupancy. Therefore, data augmentation is essential to utilize a small number
122 of image data for deep learning. Data augmentation should be designed with consideration for
123 the characteristics of images captured by the UAV. The YOLO network, which is one of the
124 deep learning algorithms, was used with the augmented data to predict the occupancy level of
125 cornfield in the images.

126
127 ***Correcting training images***

128 The cornfield images in Figure 2 show two types of distortion. The first distortion is a convex
129 fish-eye image caused by the wide-angle lens of the camera. The second distortion is due to the
130 camera not being able to capture the cornfield at the exact center position and height, resulting
131 in unequal sizes of the cornfield on the left and right sides. Therefore, it was necessary to
132 correct for the distortions to accurately compare the extent of corn occupancy in the ten images.
133 The fish-eye distortion was corrected using the method proposed by Scaramuzza [15].

134 By the way, the external and internal parameters of the camera had to be obtained to
135 connect 3D world coordinates to a 2D image. World coordinate points were selected in the
136 distorted fish-eye image and converted into camera coordinates using the external parameters.
137 The camera coordinates are then mapped onto the image plane using the internal parameters.
138 The distorted images captured from an inaccurate position and height of the UAV were solved
139 by converting them into bird-eye views which are created using inverse perspective mapping
140 to generate a 2D image of the scene. Figure 3 represents the process of correcting the image.
141 Figure 3(a) shows the distorted original image, Figure 3(b) is an example of converting the
142 fish-eye image into an undistorted image, and Figure 3(c) represents the result of correction

143 using the bird's eye view with the first corrected image (Figure 3(b)). However, it was difficult
144 to achieve perfect image correction due to the uncertainty of the camera's internal and external
145 parameters. The corrected images were cropped to a resolution of 3,520×1,760 pixels to
146 facilitate image comparison.

147

148 ***Training data***

149 Ten corrected images are very insufficient to train a deep learning network. Deep learning
150 systems based on deep artificial neural networks are highly dependent on the number of
151 training data for their performance. The large number of training data prevents overfitting of
152 prediction performance, and improves the generalization capability of the model, thereby
153 improving object detection performance. Geometric methods, such as flipping and rotating
154 images, and color adjustment methods are the most commonly used techniques for data
155 augmentation in deep learning systems [16-17].

156 Although the number of images obtained through aerial photography is very small, the
157 image resolution is still very high at 3,584×1,792 pixels even after image correction. If a high-
158 resolution image is input to the deep learning network, the number of input parameters of the
159 network increases, requiring a very long training and processing time. In addition, despite the
160 high resolution of the images, the corn plants, which are our object of interest, have very small
161 pixel sizes, making it very difficult to select the objects accurately. Therefore, it is useful to
162 divide the high-resolution images into appropriate sizes for network training, and then
163 reassemble the network's results for the segmented images for further processing. Therefore,
164 the ten corrected images were segmented into sizes suitable for deep learning in this study.

165 The actual size of the experimental subject, the corn field, is 100×50 m². Therefore, it was
166 divided into eight parts horizontally and four parts vertically at intervals of 12.5m, resulting in
167 32 images with a resolution of 448×448 pixels, as shown in Figure 4. Figure 5 shows 43 raw

168 training images selected randomly out of 320 segmented images, each with different degrees
169 of corn devastation.

170

171 **Data labels**

172 Data labels are required for training deep learning networks. The images of the cornfield were
173 labeled into three categories based on the state of the corn: $Corn_I$, $Corn_D$, $Corn_S$.

174 $Corn_I$ refers to the preserved state of corn that had not been eaten or damaged by sows. This
175 state is characterized by a clear green color of the corn, without any bending caused by sow
176 movement. $Corn_D$ refers to the state of corn that had been damaged by sows, with corn lying at
177 an angle or in a withering state. $Corn_S$ refers to the severely damaged state of corn where sows
178 had almost completely eaten the corn, leaving only the cob. Table 2 defines these three labels.

179 The raw training images were converted into data using the three defined labels based on
180 the state and size of the corn, as determined by human observation. The sample in Table 2
181 shows an example of the 43 images. The definition for each labeled bounding box is as shown
182 in Equation (1).

$$183 \quad Box_{ij}(Bx_{ij}, By_{ij}, Bw_{ij}, Bh_{ij}) \quad (1)$$

184 where, i denotes the label index, j denotes the bounding box number, (Bx_{ij}, By_{ij}) represents
185 the coordinates of the top-left corner of the bounding box, and (Bw_{ij}, Bh_{ij}) represents the
186 width and height of the bounding box.

187

188 **Data augmentation**

189 Data augmentation is a method of increasing the size of a dataset by generating new data that
190 reflects the characteristics of the original data, especially in cases where the original dataset is
191 limited. Although we have created 43 basic datasets for image segmentation and data labeling,

192 it is still a very small number for training deep learning networks. Images obtained from the
193 UAV are particularly advantageous for data augmentation techniques such as rotating or
194 flipping images to increase data. In general, small angles are commonly used when performing
195 data augmentation by rotation transformation. For example, an image of a person rotated by
196 180 degrees is not needed as a training image. On the other hand, it is irrelevant even if the
197 image is rotated by 180° for corn images captured by UAVs. Furthermore, flipped images (both
198 horizontally and vertically) can also be used as training images.

199 To effectively increase the number of training images, the 43 original data images were
200 flipped to create 86 images, and then these images were further augmented by rotating them in
201 5-degree increments to create a total of 6,192 images. The increased 6192 images are further
202 augmented by applying three random color transformations to each image, resulting in a total
203 of 24,768 datasets. Figure 5 represents this process described above.

205 ***YOLOv4 Object Detection and Network Training***

206 Figure 7 shows the YOLOv4 object detector used in this study to recognize the degree of corn
207 devastation. In this study, ResNet50 was used as a backbone for detecting object characteristics,
208 and SPP (Spatial Pyramid Pooling) and PANet (Path Augmented Network) were applied to the
209 neck. The head was the same as YOLOv3. The output of the head represents the position and
210 size of the bounding box, the probability of confidence score on the object, and the probability
211 of class. The final output of YOLOv4 selects the final bounding boxes by applying the output
212 values of the head and the non-maximum suppression (NMS). The input of the YOLOv4
213 detector is an image with 448×448 pixels. After correction, the image is divided into 32 (4×8)
214 segments and inputted into the YOLOv4 detector. YOLOv4 extracts the features of the corn
215 image when the image is inputted, and outputs the position and size of the corn image as well
216 as the probability of each class.

217 The YOLOv4 network used in this study was provided by Matlab[®] [18], and the backbone
218 network was changed by modifying the input layer of the network to match the augmented
219 dataset using ResNet50. For the training parameters, the initial training rate was set to 0.001,
220 and Adam Optimizer was used for the training method. The network was trained for a
221 maximum of 30 epochs with a mini-batch size of 32. The hardware used in the study includes
222 the Intel i9-12900 central processing unit and NVIDIA RTX-A6000 graphics accelerator.

223 The YOLOv4 network uses anchor boxes with specific heights and widths of predefined
224 bounding boxes to improve the efficiency and object detection performance of the network,
225 which also has a significant impact on training time. To determine the number of specific
226 bounding boxes, the average IoU (Intersection over Union) value was calculated for all the
227 bounding boxes in the prepared dataset, and the optimal value was selected. Figure 8 shows
228 the average IoU value for all bounding boxes in the dataset by the number of specific boxes.
229 The average IoU value is high at 0.86 when the number of specific boxes is 4.

230 The total loss function used for training the YOLOv4 network is equation (2), where the
231 object classification loss and object confidence loss are computed using binary cross-entropy,
232 and the bounding box localization error is computed using the Root Mean Square Error
233 (RMSE).

$$234 \quad TotalLoss = a \times clsloss + b \times objloss + c \times boxloss \quad (2)$$

235 where, $[a, b, c] = [1, 1, 1]$ represents the weights for each loss term, where *clsloss* is the
236 object classification loss, *objloss* is the object confidence loss, and *boxloss* is the bounding
237 box localization error.

238 The YOLOv4 network reached a RMSE of 0.21 after 30 epochs of training. Figure 8
239 shows some of the results of YOLOv4 network after training on 24,768 images.

240

241 ***Estimating the distribution and occupancy of corn***

242 The proposed system aims to estimate the distribution and occupancy of corn for a specific
 243 date using a YOLOv4 network trained on a dataset of 24,768 images generated through data
 244 augmentation. Figure 10 shows an overview of the proposed overall system using a corn
 245 image for a specific date. As the input of the trained YOLOv4 detector is a 448×448 pixel
 246 image, the captured image for a specific date is corrected to 3,584×1,792 pixels and then
 247 sequentially inputted into the YOLOv4 detector by dividing it into 32 (4×8) segments. When
 248 an image is inputted into YOLOv4, it extracts features of the corn image and calculates the
 249 location and size of the corn in the image, as well as the probability of an object existing and
 250 the class probability. Objects with a probability of existence and a class probability above a
 251 certain threshold are selected for bounding boxes by NMS. For each segmented image, the
 252 number and area of labels detected by YOLOv4 are accumulated and calculated. As YOLOv4
 253 outputs the location and size of corn in the image, the occupancy rate is calculated using
 254 Equation (3) by setting weights based on the three states of corn.

$$Occupancy_i = \left(w_1 \times \sum_{j=1}^{32} \sum ACorn_{I,ij} + w_2 \times \sum_{j=1}^{32} \sum ACorn_{D,ij} + w_3 \times \sum_{j=1}^{32} \sum ACorn_{S,ij} \right) / Max_{ACorn} \quad (3)$$

256 where, $i = 1, 2, \dots, 10$ represents the index of the corn field image and $j = 1, 2, \dots, 32$ represents
 257 the segmented image. w_1, w_2, w_3 are the weights assigned to each state of corn. $ACorn_{I,ij}$
 258 represents the area of $Corn_I$, $ACorn_{D,ij}$ represents the area of $Corn_D$, and $ACorn_{S,ij}$ represents
 259 the area of $Corn_S$. Max_{ACorn} represents the maximum area of corn occupancy.

261 **RESULTS**

262 Figure 11 shows the detection results of the images captured 10 times in chronological order.
263 Figure 11(a) shows the number and total area of intact corn objects represented by $Corn_I$
264 without being damaged by sows. It can be seen that it decreases exponentially over time. Figure
265 11(b) represents the number and total area of corn plants $Corn_D$. It can be seen that it linearly
266 increases until the fourth day, and then decreases afterward. Figure 11(c) represents the number
267 and total area of corn plants $Corn_S$. It can be seen that it sharply increases until the fourth day
268 and gradually decreases afterward similar to the results of $Corn_D$. Figure 11(d) represents the
269 occupancy rate of corn plants calculated using Equation (3). The weights for corn plant
270 conditions were set as $[w_1, w_2, w_3] = [1, 0.5, 0.2]$, and the date with the largest area of land was
271 set as the second day because no image was taken on the first day when the sow was released
272 into the pasture. It can be seen that the occupancy rate of corn plants decreases very rapidly
273 over time.

274 As a result, the occupancy rate of corn in the field was estimated efficiently using YOLO.
275 As of the first day of observation (day 2), it was evident that almost all the corn had disappeared
276 by the ninth day. When grazing 20 sows in a $50 \times 100 \text{ m}^2$ cornfield ($250 \text{ m}^2/\text{sow}$), it appears that
277 the animals should be rotated to other grazing areas to protect the cover crop after at least five
278 days.

279

280 **DISCUSSION**

281 **YOLO object detection system**

282 The input image was divided into grid cells through CNN, and objects are detected by
283 generating anchor boxes and class probabilities for each cell section to predict the object's
284 location and size [19]. Anchor boxes are boundary boxes with predefined height and width,
285 and they are much faster than other detection systems because they do not use a separate

286 network to extract candidate regions, unlike two-stage detectors. The YOLO object detection
287 system has been improved by many researchers, and YOLOv4 demonstrates faster and more
288 accurate detection rates among various versions by incorporating state-of-the-art deep learning
289 techniques such as Weighted Residual Connections (WRC), Cross Stage Partial Connections
290 (CSP), and the Complete Intersection over Union (CioU) loss [20]. The YOLOv4 network
291 consists of a backbone network and a neck to detect object features, and the head outputs the
292 object's position, the probability of being on the object, and the class probabilities. The final
293 objects were detected by applying this.

294 Recently, image and video processing techniques have been widely applied in various
295 fields, especially in the field of computer vision, where there has been significant research on
296 image classification, object detection, and multiple object detection within images. As a
297 classical image processing method, the image processing-based approach classifies and
298 recognizes objects based on their direct features such as color, texture, and edges. This
299 approach often results in significantly different output in object recognition within images due
300 to lighting conditions, shadows, and camera settings.

301 For several years, object detection research in image recognition using machine and deep
302 learning techniques has demonstrated significant advantages in computer vision tasks, resulting
303 in significant improvements in object detection and recognition performance compared to
304 traditional approaches [21]. This progress has been made possible by the utilization of big data,
305 advances in high-performance hardware such as Graphic Processing Units (GPUs), and the
306 development of useful learning algorithms for deep learning training, which has led to the
307 evolution of practical and useful technologies.

308 The CNN(Convolutional Neural Network) is the most widely used deep learning
309 algorithm for object detection research and was developed by LeCun in the late 1990s, which
310 has a very high accuracy in object detection compared to traditional image processing methods

311 [22]. In addition to CNN, YOLO is widely used in object detection research due to its fast-
312 processing time and high accuracy. Many studies have been conducted on YOLO in object
313 recognition [10]. However, CNN requires algorithms such as Region-CNN (RCNN) to
314 recognize the exact location of objects within an image in addition to object detection [23].
315 However, while RCNN has improved the accuracy of object detection, it requires a lot of
316 computational time compared to traditional image processing methods and has an extremely
317 high complexity of network training and algorithm.

318 On the other hand, YOLO has fast object detection and high accuracy. Machine and deep
319 learning-based farming technologies are mainly applied for fruit detection and ripeness
320 classification, as well as predicting pests and diseases in fruits [19]. In early machine learning
321 research, Quiang et al. [24] identified fruits and tree branches using an SVM (Support Vector
322 Machine) trained in the RGB color space. While it showed superior performance compared to
323 previous threshold-based methods, it is still heavily affected by lighting conditions. Zhao et al.
324 [25] applied a combination of the AdaBoost classifier and color analysis for tomato detection,
325 but real-time processing was difficult due to the slow processing speed. Luo et al. [26] also
326 suggested an AdaBoost and color feature-based framework for grapefruit detection, but it was
327 affected by weather conditions and changes in lighting such as leaf covering.

328 Traditional machine learning research has greatly improved image processing-based
329 methods, but the design of proposed methods is complicated and only adaptable to some
330 specific conditions, resulting in poor flexibility. Deep learning has overcome the limitations of
331 traditional machine learning by being more abstract and generalizable, particularly through the
332 use of CNNs. Additionally, the utilization of big data has made it possible to apply these
333 technologies to a range of agricultural problems, including image processing. Sa et al. [27]
334 applied Faster R-CNN [28] to RGB and near-infrared images for fruit detection and showed
335 better performance than previous methods. Mota-Delfin et al. [11] used YOLO to detect corn

336 effectively in a weed-rich background using images captured by RPAS (Remotely Piloted
337 Aerial Systems) and predicted the yield [10].

338 The basic data augmentation techniques include image processing methods that preserve
339 the characteristics of the original image while maintaining diverse features of the objects. There
340 are image processing techniques such as flipping, rotating, cropping images, and adjusting their
341 brightness and color using various methods [16].

342

343 **CONCLUSION**

344 In agricultural technology, most of the research using machine and deep learning is related to
345 the detection of fruits and pests, and research on other application fields is needed. In addition,
346 large-scale image data collected by experts in the field are required as training data to apply
347 deep learning. However, collecting training data takes a lot of time and effort. If there are few
348 images for training, the effort and time for acquiring training images can be reduced while
349 increasing training images through image segmentation and data augmentation (flip, rotation,
350 brightness, color adjustment conversion) as in the proposed method. In addition, calculating
351 the occupancy level of the whole image after calculating the occupancy level of each segmented
352 image, as in the proposed method, is very effective. It is an excellent and effective technique
353 to classify the status of corn ($Corn_I$, $Corn_D$, $Corn_S$) by date using the YOLO network.
354 Therefore, the proposed method can be easily applied to many other fields and guarantees high
355 precision.

356

357 **CONFLICT OF INTEREST**

358 We certify that there is no conflict of interest with any financial organization regarding the
359 material discussed in the manuscript.

360

361 **REFERENCES**

- 362 1. Jang JC, Oh SH. Management factors affecting gestating sows' welfare in group housing
363 systems - A review. *Anim Biosci* 2022;35(12): 1817-1826.
- 364 2. Choi W, Nassif N, Whitley NC, Oh SH. Comparison of temperature susceptibility for three
365 types of outdoor farrowing huts. *Applied Engineering in Agriculture* 2014;30(2): 241-247.
- 366 3. Park H, Min B, Oh SH. Research trends in outdoor pig production. *Animal Bioscience*
367 2017a;30(9):1207-1214.
- 368 4. Park H, Oh SH. Seasonal variation in growth of Berkshire pigs in alternative production
369 systems. *Animal Bioscience* 2017b;30(5):749-754.
- 370 5. NRCS. 2007. Conservation planning guidelines for outdoor swine operations.
- 371 6. Pietrosemoli S, Green J, Bordeaux C, Menius L, Curtis J. 2012. Conservation practices in
372 outdoor hog production systems: Findings and recommendations from the Center for
373 Environmental Farming Systems. Center For Environmental Farming Systems, North
374 Carolina State University.
- 375 7. Whitley N, Hanson D, Morrow WEM, See MT, Oh SH. Comparison of pork quality and
376 sensory characteristics for antibiotic free Yorkshire crossbreds raised in hoop houses. *Animal*
377 *Bioscience* 2012a;25(11):1634-1640.
- 378 8. Whitley N, Morrow WEM, See MT, Oh SH. 2012b. Comparison of growth performance in
379 antibiotic-free Yorkshire crossbreds sired by Berkshire, Large Black, and Tamworth breeds
380 raised in hoop structures. *Animal Bioscience* 2012b;25(10):1351-1356.
- 381 9. Lee JM, Lee YH, Choi NK, Park H, Kim HC. Deep-Learning-based plant anomaly detection
382 using a drone. *Journal of the Semiconductor & Display Technology* 2021;20(1):94-98.
- 383 10. Redmon J, Divvala S, Girshick R, Farhadi A. You only look once: Unified, real-time object
384 detection. *Proceedings of the IEEE conference on computer vision and pattern recognition.*
385 2016;779-788. 10.1109/CVPR.2016.91
- 386 11. Mota-Delfin C, López-Canteñs G, López-Cruz IL, Romantchik-Kriuchkova E, Olguín-
387 Rojas JC. Detection and counting of corn plants in the presence of weeds with convolutional
388 neural networks. *Remote Sensing.* 2022;14(19):4892. doi.org/10.3390/rs14194892.

- 389 12. Du J. Understanding of object detection based on CNN family and YOLO. J Physics:
390 Conference Series. 2018. IOP Publishing.
- 391 13. Viswanatha V, Chandana R, Ramachandra A. Real time object detection system with YOLO
392 and CNN Models: A Review. J Xi'an Univ Archit Technol. 2022;14(7):144-151.
- 393 14. Tabelini L, Berriel R, Paixao TM, Badue C, De Souza AF, Oliveira-Santos T. Keep your
394 eyes on the lane: Real-time attention-guided lane detection. Proceedings of the IEEE/CVF
395 conference on computer vision and pattern recognition. 2021.
- 396 15. Scaramuzza D, Martinelli A, Siegwart R. A toolbox for easily calibrating omnidirectional
397 cameras. Proceeding to IEEE International Conference on Intelligent Robots and Systems.
398 IEEE. 2006.
- 399 16. Shorten C, Khoshgoftaar TM. A survey on image data augmentation for deep learning.
400 Journal of big data, 2019;6(1):1-48.
- 401 17. Taylor L, Nitschke G. Improving deep learning with generic data augmentation. in 2018
402 IEEE Symposium Series on Computational Intelligence (SSCI). 2018.
- 403 18. Works TM. Lidar object detection using complex-YOLO v4 Network. 2022.
- 404 19. Kamilaris A, Prenafeta-Boldú FX. Deep learning in agriculture: A survey. Computers and
405 Electronics in Agriculture. 2018;147:70-90.
- 406 20. Bochkovskiy A, Wang CY, Liao HYM. Yolov4: Optimal speed and accuracy of object
407 detection. arXiv preprint arXiv:2004.10934, 2020.
- 408 21. Voulodimos A, Doulamis N, Doulamis A, Protopapadakis E. Deep learning for computer
409 vision: a brief review. Comput Intell Neurosci 2018;7068349.
- 410 22. LeCun Y, Bottou L, Bengio Y, Haffner P. Gradient-based learning applied to document
411 recognition. Proceedings of the IEEE, 1998;86(11):2278-2324.
- 412 23. Girshick R, Donahue J, Darrell T, Malik J. Rich feature hierarchies for accurate object
413 detection and semantic segmentation. Proceedings of the IEEE conference on computer
414 vision and pattern recognition. 2014;580-587. 10.1109/CVPR.2014.81
- 415 24. Qiang L, Jianrong C, Bin L, Lie D, Yajing Z. Identification of fruit and branch in natural
416 scenes for citrus harvesting robot using machine vision and support vector machine. Int J

417 Agric Biol Eng. 2014;7(2):115-121.

418 25. Zhao Y, Gong L, Zhou B, Huang Y, Liu C. Detecting tomatoes in greenhouse scenes by
419 combining AdaBoost classifier and colour analysis. Biosyst Eng. 2016;148:127-137.

420 26. Luo L, Tang Y, Zou X, Wang C, Zhang P, Feng W. Robust grape cluster detection in a
421 vineyard by combining the AdaBoost framework and multiple color components. Sensors.
422 2016;16(12):2098.

423 27. Sa I, Ge Z, Dayoub F, Upcroft B, Perez T, McCool C. Deepfruits: A fruit detection system
424 using deep neural networks. Sensors. 2016;16(8):1222.

425 28. Ren S, He K, Girshick R, Sun J. Faster r-cnn: Towards real-time object detection with
426 region proposal networks. IEEE Transactions on Pattern Analysis and Machine Intelligence.
427 2017;39(6):1137-1149. 10.1109/TPAMI.2016.2577031 28.

428

ACCEPTED

429 **Table 1.** Specifications of the UAV platform used in the study.

Airframe	DJI Phantom 2 Quad-rotor
Dimensions	43.2 x 20.6 x 31.75 cm
Battery	3S LiPo 5200mAh, 11.1V
Takeoff Weight	≤1300g
Maximum Flight Time	25min (approx.)
Signal Frequency	2.4GHz ISM
Diagonal Length	350mm


430

431

ACCEPTED

432

433 **Table 2.** Data labels

Label	Label index	Color	Corn description	Sample
$Corn_I$	0	Blue	Intact corn	
$Corn_D$	1	Yellow	Damaged corn	
$Corn_S$	2	Red	Corn with stubble	

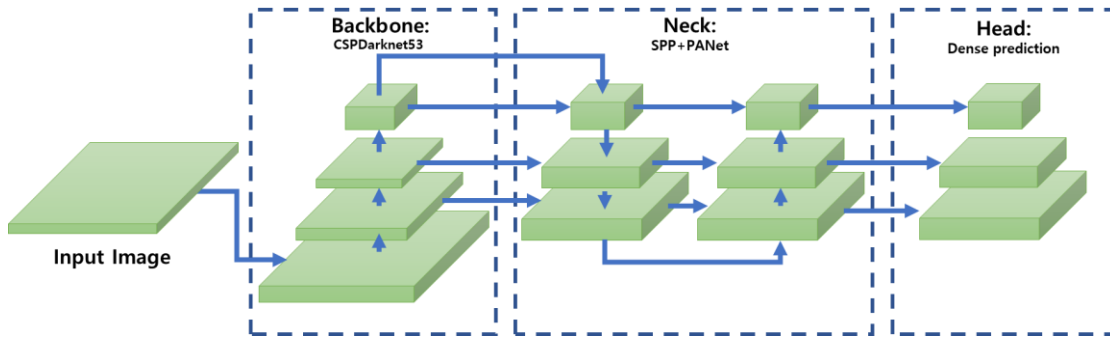
434

435

436

ACCEPTED

437
438



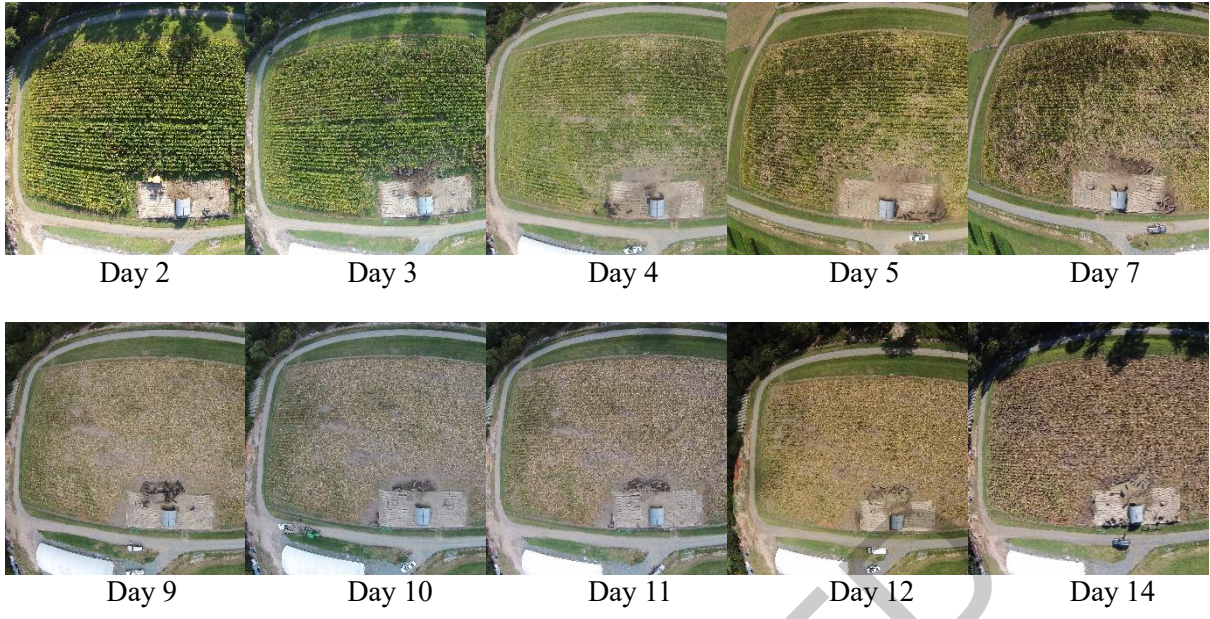
439

440

Figure 1. The YOLO Detection System

441

ACCEPTED



442
443
444

Figure 2. Original images used for the analysis

ACCEPTED

445
446
447
448
449
450
451
452
453
454
455
456
457
458
459
460

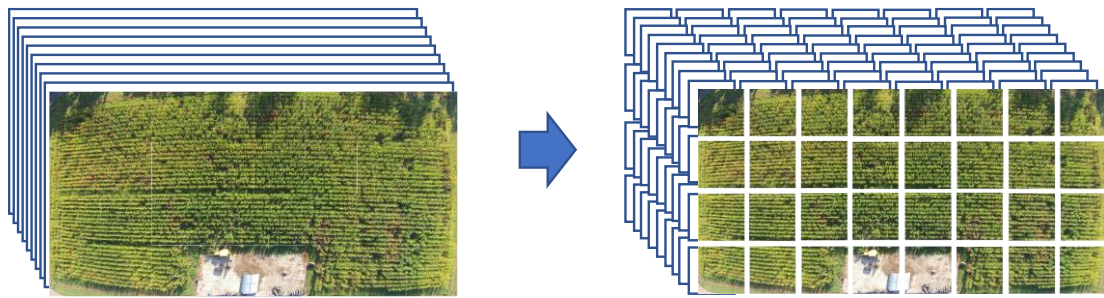


2 (a) Distorted image (b) Undistorted image (c) Bird's eye view and cropping

3 **Figure 3.** Example of image correction

ACCEPTED

461



462

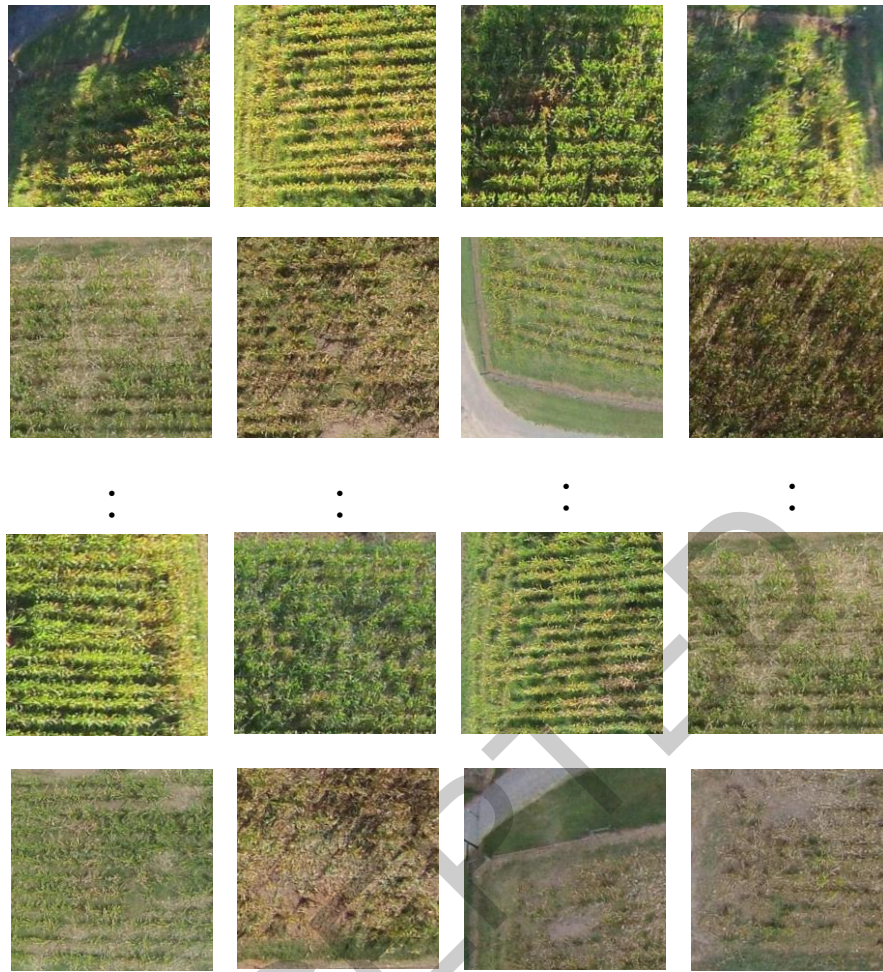
463

Figure 4. 4×8 split images

464

465

ACCEPTED



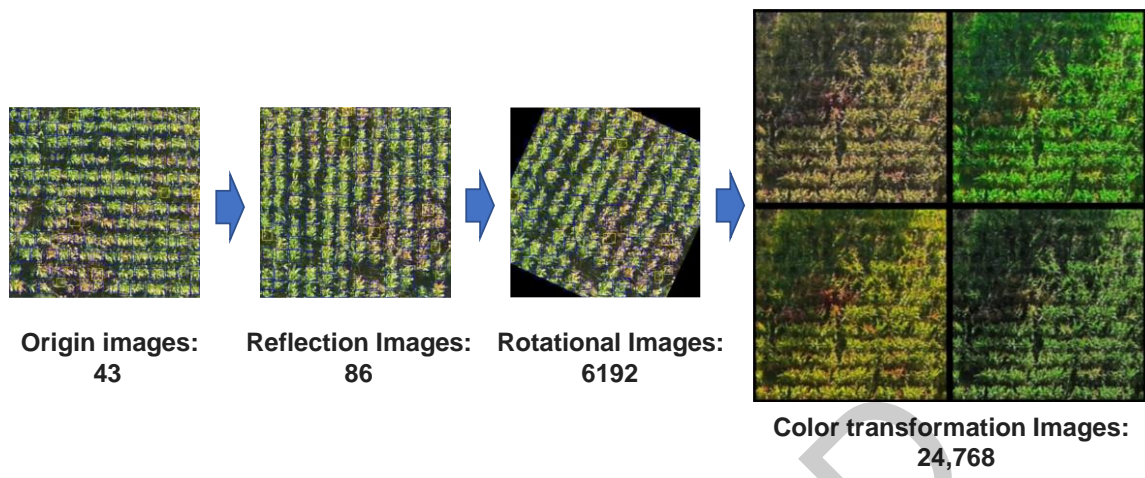
466

467

468

Figure 5. Raw training images

469



470

471

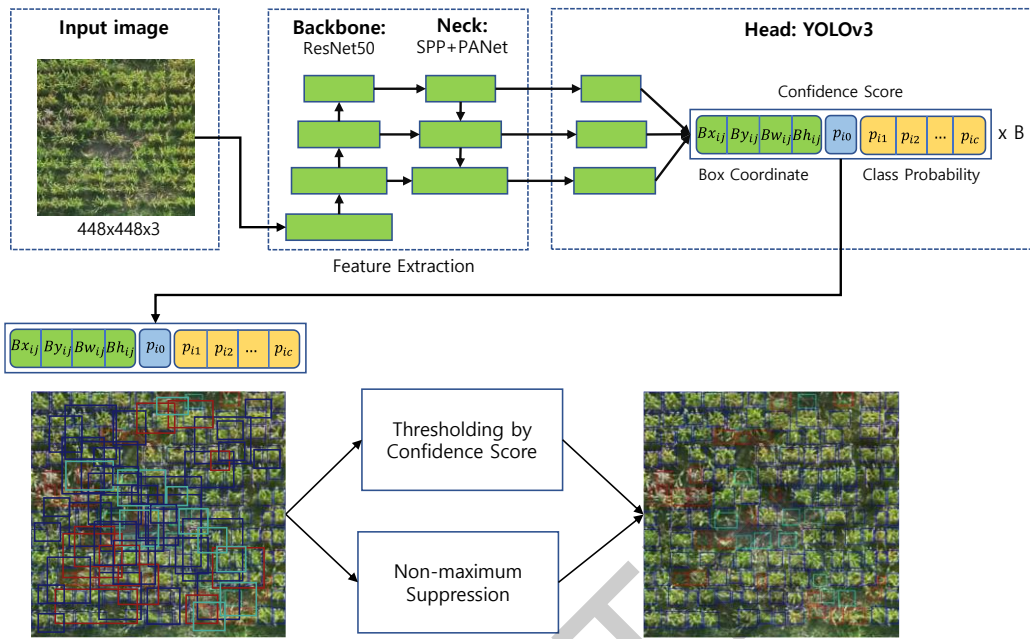
Figure 6. Data augmentation

472

473

ACCEPTED

474



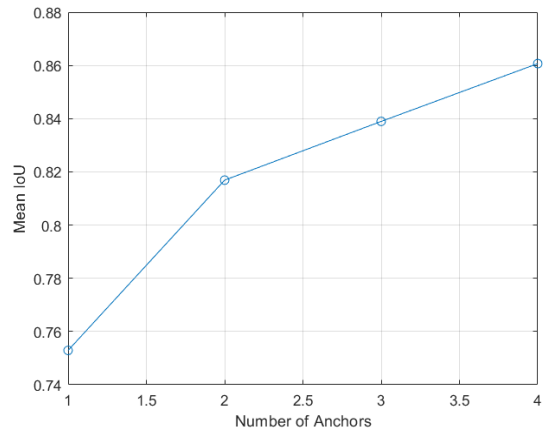
475

476

477

478

Figure 7. YOLO Detection



479

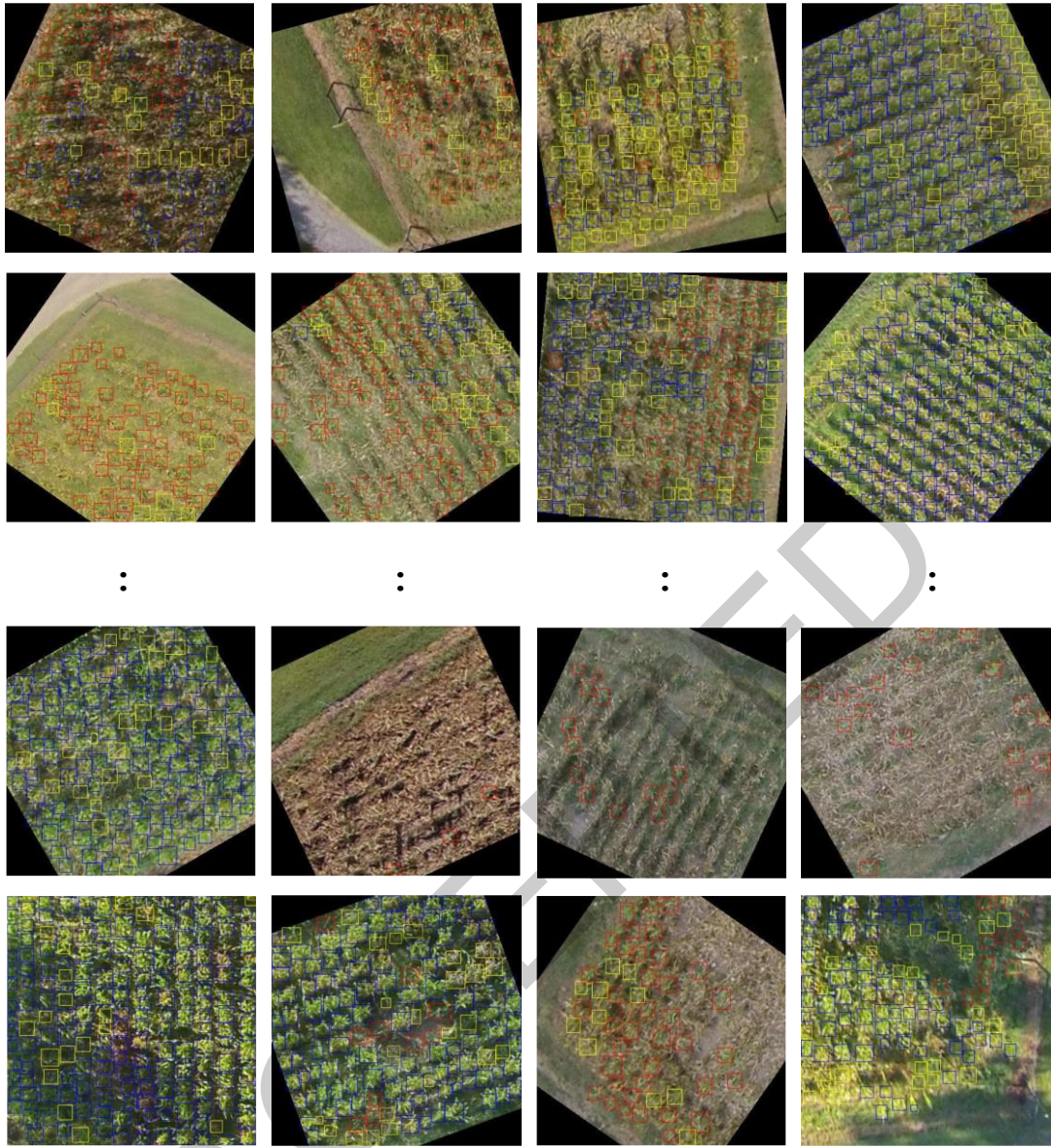
480

Figure 8. Number of Anchors vs. Mean IoU

481

482

ACCEPTED



483

484

Figure 9. Recall results after training

485

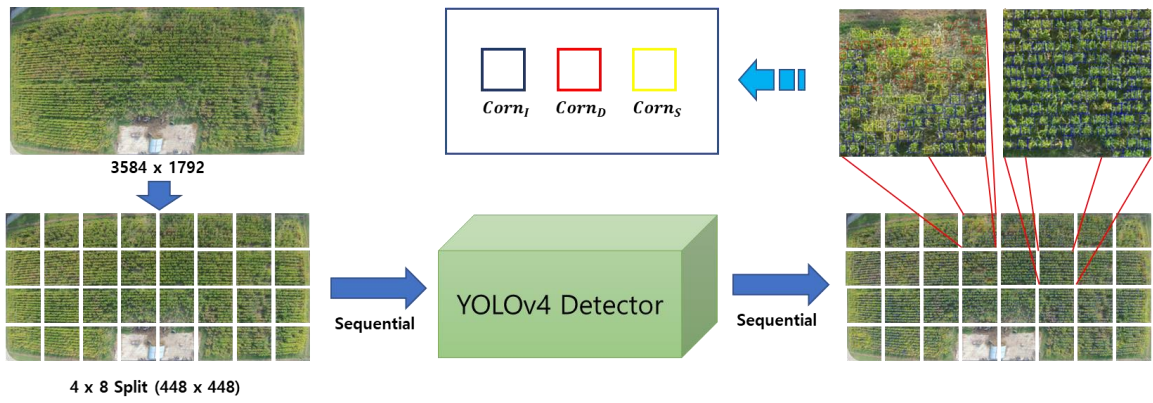
486

487

488

489

490



491

492

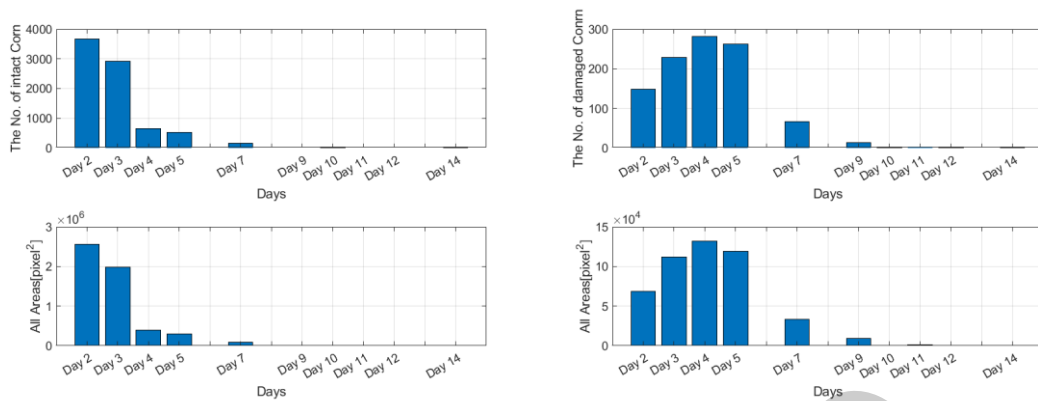
Figure 10. System configuration

493

494

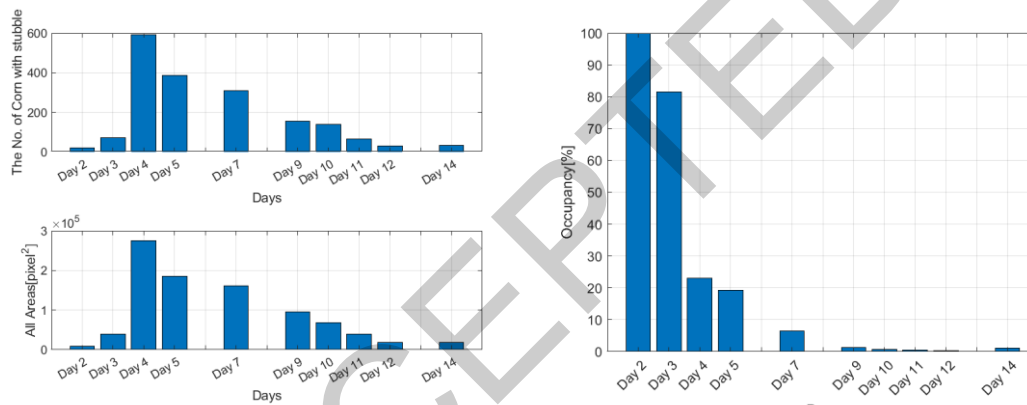
ACCEPTED

495



496
497

(a) The case of intact corn (b) The case of damaged corn



498
499

(c) The case of corn with stubble (d) The occupancy rate of corn

500

Figure 11. The degree of occupancy of corn by date

501

502

503